The Study of Relative Density and Boundary Effects for Cone Penetration Tests in Centrifuge

M. D. Bolton [1] and M. W. Gui [2]

CUED/D-SOILS/TR256 1993

1. Lecturer, Cambridge University Engineering Department, UK.
2. Research Student, Cambridge University Engineering Department, UK.

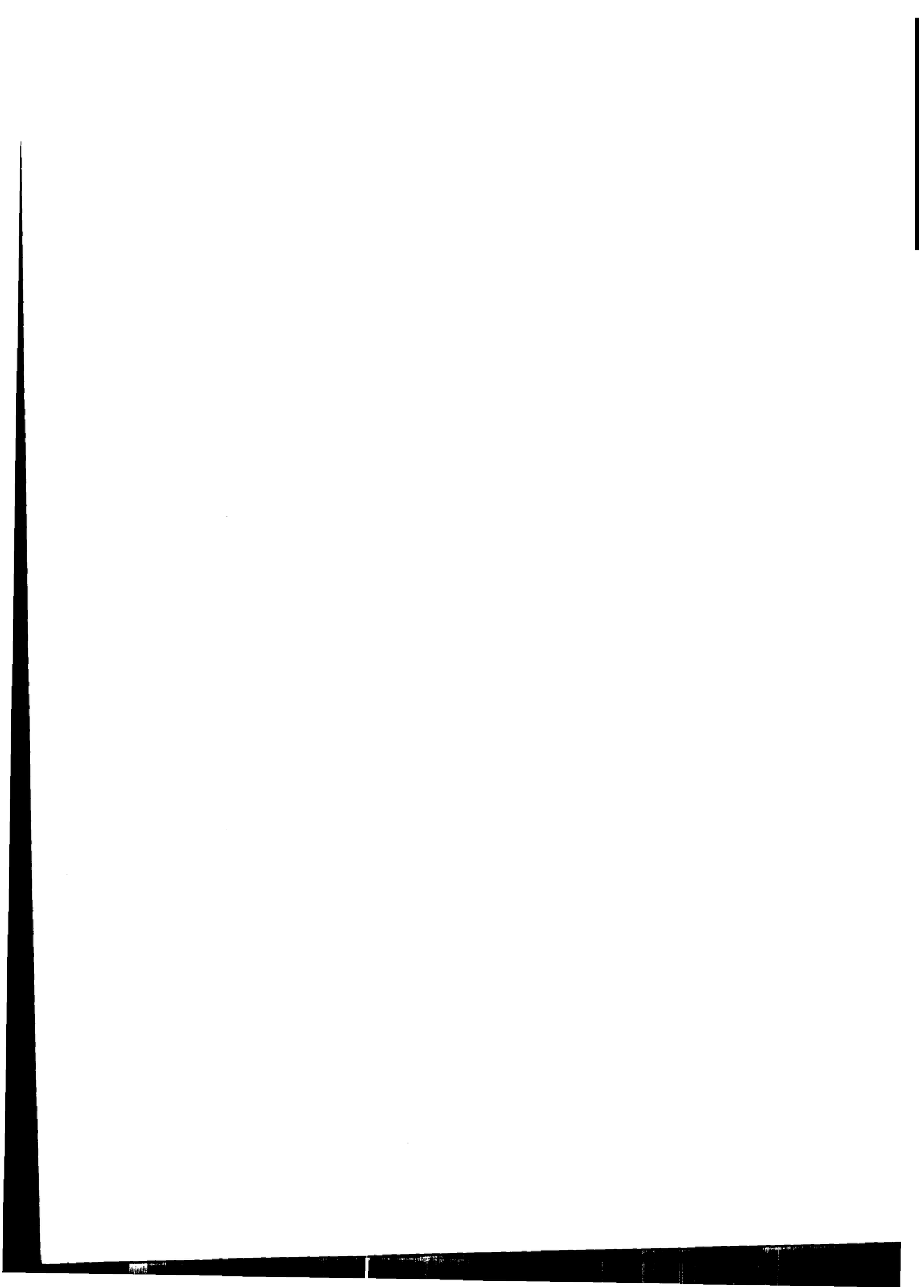

Abstract

A series of cone penetration tests were carried out at the Cambridge Geotechnical Centrifuge Centre. The tests were performed using a 10*mm* diameter cone penetrometer. In order to study the effect of diameter ratio, three different sizes of container (210*mm*, 420*mm* and 850mm diameter) were used. The repeatability of the model preparation technique using a single hole hopper was checked prior to these tests. Side boundary and base boundary effects are found to be significant and a minimum diameter ratio is proposed for tests to be carried out using a circular container. The effect of the relative density of Fontainbleau sand is studied. The possibility of simulating an infinite body of sand is also mentioned. It has also been demonstrated that the relative density of sand can be correlated with the normalised tip resistance.

Contents

List of Figures

Notation

B	=	diameter of the cone
d	=	mean particle diameter
D	=	diameter of container
g	=	earth's gravity$(9.81 m/s^2)$
I_D	=	relative density
K	=	coefficient of earth pressure
L	=	distance of cone from the total stress cell
n	=	ratio between centrifugal acceleration and earth's gravity
NC	=	normally consolidated
OC	=	overconsolidated
OCR	=	overconsolidation ratio
p'_c	=	soil particle crushing strength
P_o	=	container pressure
q_c	=	measured tip resistance
R_s	=	radius at the surface of the specimen
X	=	distance of cone from the base of the container
z_m	=	depth in the model from the surface to the specimen
z_{pc}	=	corrected prototype depth
Z	=	normalized prototype depth
ϕ_{crit}	=	critical angle of shearing
σ'_v	=	initial effective vertical stress
σ_v	=	initial total vertical stress
γ_d	=	dry density of soil
γ_w	=	density of water

1 Introduction

Cone penetration test (CPT) has been widely used in the last twenty years as an site investigation tool. It is a relatively simple test and capable of providing a continuous profile of a site. In order to obtain the engineering parameters from the raw data, laboratory calibration of CPT data, using calibration chambers, is necessary. To simulate the effect of the overburden pressure, a surcharge is used. However, the effect of stress gradient due to the self-weight of the soil cannot be simulated in this way. Hence, the results obtained from calibration chamber always leave room for questioning.

To simulate the effect of self-weight, centrifuge testing has been adopted for all sorts of geotechnical problems. A specimen of soil is prepared in a strongbox in the laboratory, instrumented and transferred carefully to the centrifuge for testing. A collaboration exists between European centrifuge centers at Bergamo, Bochum, Copenhagen, Nantes and Cambridge, to standardize methods of in-flight site investigation in centrifuge models.

Bolton et al (1993) have demonstrated the importance of having miniature probes to measure in-flight soil parameters, Therefore, a data bank for in-flight CPT will be very useful when correlations of soil parameters are required.

A series of CPT have, therefore, been conducted at the Cambridge Geotechnical Centrifuge centre. The objective of this report is to study the effects of the relative density I_D, the diameter ratio $\frac{D}{B}$ (container diameter to the cone diameter), and the similar base boundary effect, on the tip resistance q_c of CPT. For this purpose, the cone tip resistance q_c is normalised with respect to overburden pressure, and the current depth is normalised with respect to cone diameter.

2 Literature Review

Hitherto, except for Ferguson and Ko (1981), Phillips and Valsangkar (1987) and Lee (1990), most of the cone data were calibrated from calibration chambers. Different boundary conditions in calibration chambers can be simulated by varying the lateral pressures around the circumference of the chamber via a rubber membrane. In order to study the

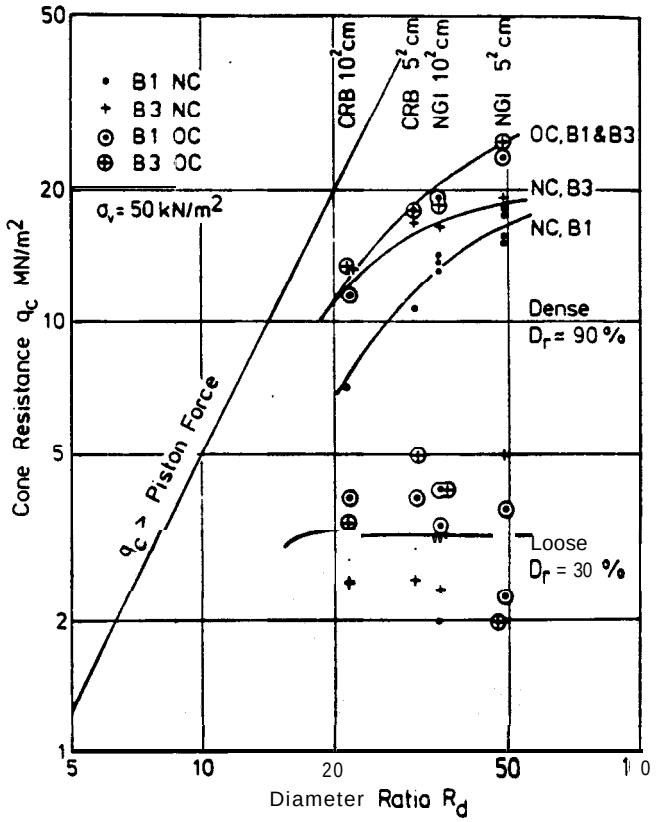

Figure 1: Chamber size effects on q_c (after Parkin & Lunne, 1982)

boundary effects, different sizes of calibration chamber and different diameters of cone were adopted. The boundary effects for calibration chamber tests have been studied by some researchers (eg. Last (1979), Parkin & Lunne (1982) and Ghiona (1984)) and are summarised in the following section.

2.1 Calibration chamber tests

Parkin and Lunne (1982) investigated boundary effects in flexible-walled chambers. The tests were preformed using cones with different diameters B in calibration chambers with different sizes D. The boundary conditions on the flexible side and base were either constant volume $B3$ or constant stress $B1$ and the results were plotted in terms of tip resistance q_c and diameter ratio $(\frac{D}{B})$ in Fig ll. It was concluded that for loose sand $(I_D = 15 - 30\%)$, the boundary effects are negligible and for NC dense sand $(I_D = 90\%)$, a diameter ratio of about 50 is desirable in order to eliminate the boundary effects.

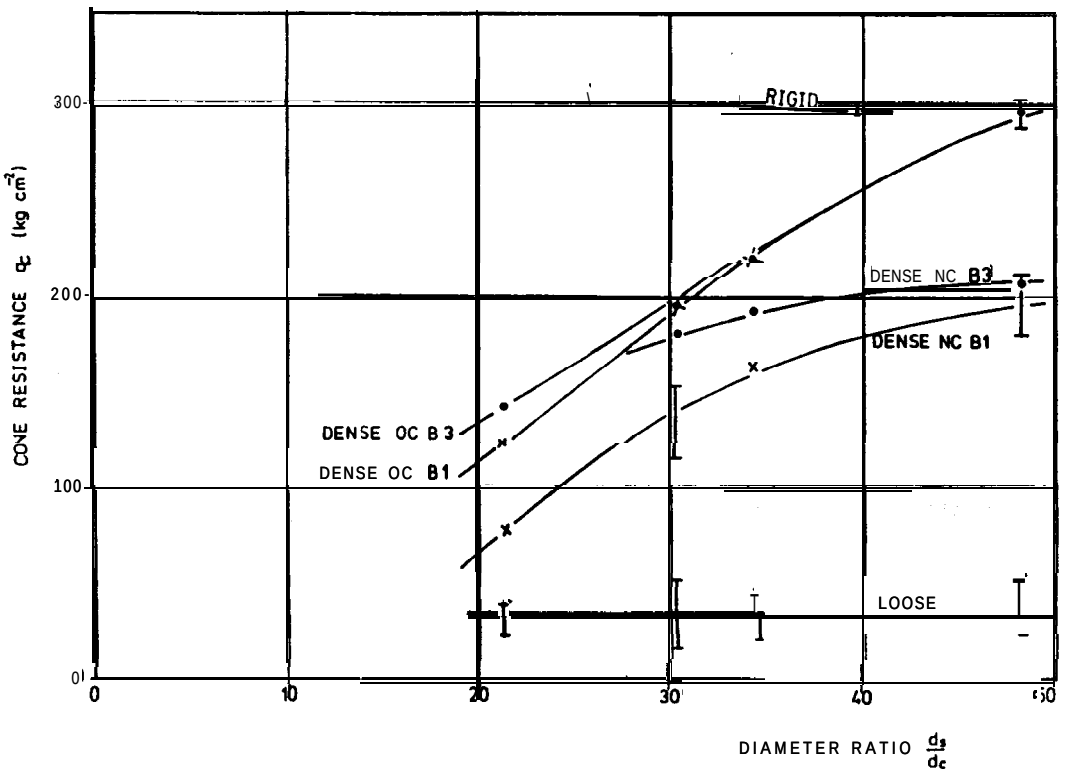

Figure 2: Variation of q_c with diameter ratio (after Last, 1979)

Two phenomenons have also been observed by the authors :

1. In the constant volume tests B3 on NC sand, peneteration caused the coefficient of earth pressure K to rise, leading to higher q_c, as compared to constant stress tests $B1$.

2. This phenomenon was not observed for OC sand because K value was initially near 1 so that large increases cannot be sustained.

The experimental results performed by Last (1979) in a rigid-walled concrete chamber were also reported by Parkin and Lunne (1982). The diameter ratios in this study were 28.0 and 39.7. The q_c values as plotted in Fig 2 , were to the surprise of Parkin and Lunne (1982) - no higher than those obtained with flexible boundaries. Parkin and Lunne (1982) attributed this to the friction mobilized on the rigid side walls which resulted in a lower ambient stress in the centre of the sample, Fig 3 .

Ghiona (1984) showed that for dense Ticino sand ($I_D = 90\%$), there was no chamber size effect as observed by Parkin and Lunne (1982). The only explanation offered was that the material was different from the one used by Parkin and Lunne (1982).

Phillips and Valsangkar (1987) carried out CPT on Fontainbleau and Leighton Buzzard 14/25 sands ($I_D = 87\%$) in a 850mm diameter tub. The results of the tests using a cone with B = 10mm at distance ratios of 10B, 20B and 42B and tests using a cone with B = 20mm at distance ratios of 5B, 10B and 21B are presented in Fig 4 (a) & (b).

It was concluded that side wall boundary effects are negligible in the current centrifuge setup. Small variations in the test results may be due to stress cycling caused by stoppage of centrifuge between tests. However, Phillips and Valsangkar (1987) recommended that care has to be taken in extrapolating cone results when more than one side-wall is close to the penetrometer.

2.2 Some remarks about calibration chamber tests

There are some uncertainties for the tests performed in the calibraton chambers :

1. Parkin and Lunne (1982) observed the variation of container pressure, P_o, throughout the penetration test. If they normalised q_c with respect to P_o and plotted $\frac{q_c}{P_o}$ instead, would they have observed any normalised boundary effect ?

2. Constant volume in a triaxial cell chamber does not mean zero strain everywhere ($\epsilon_r \neq 0$). Hence, "constant volume" chamber tests will be much more compliant at the boundary than centrifuge tests.

3. The data obtained by Last (1979) and Parkin and Lunne (1982) seem not to explain $q_c = f(z_{pc})$ very convincingly, Fig 3. It is believed that the initial portion of the curve could be due to the top boundary effect.

4. For tests carried out in a flexible-walled chamber, the constant stress boundary condition $B1$ will underestimate q_c as higher values will develop in the field or centrifuge at the equivalent distance from the cone.

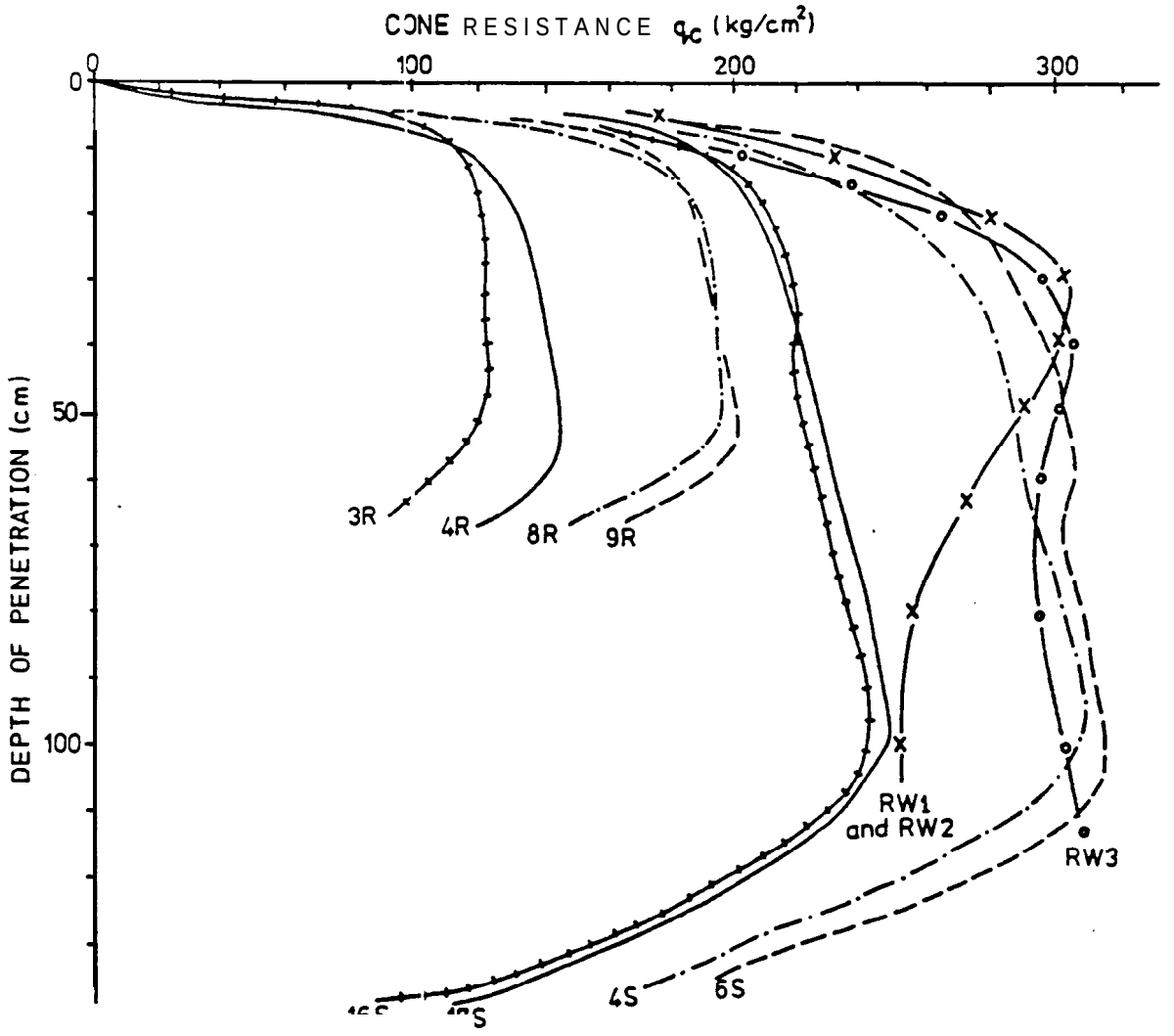

TEST	PENETROMETER (cm)	BOUNDARY CONDITION
3R	10	B1
4R	10	B3
8R	5	B1
9R	5	B3
4S	5	B1
6S	5	B3
16S	10	B1
17S	10	B3
RW1, RW2	5	RIGID
RW3	10	RIGID

Figure 3: Comparison of q_c profiles for OC sand in calibration and rigid-walled chambers

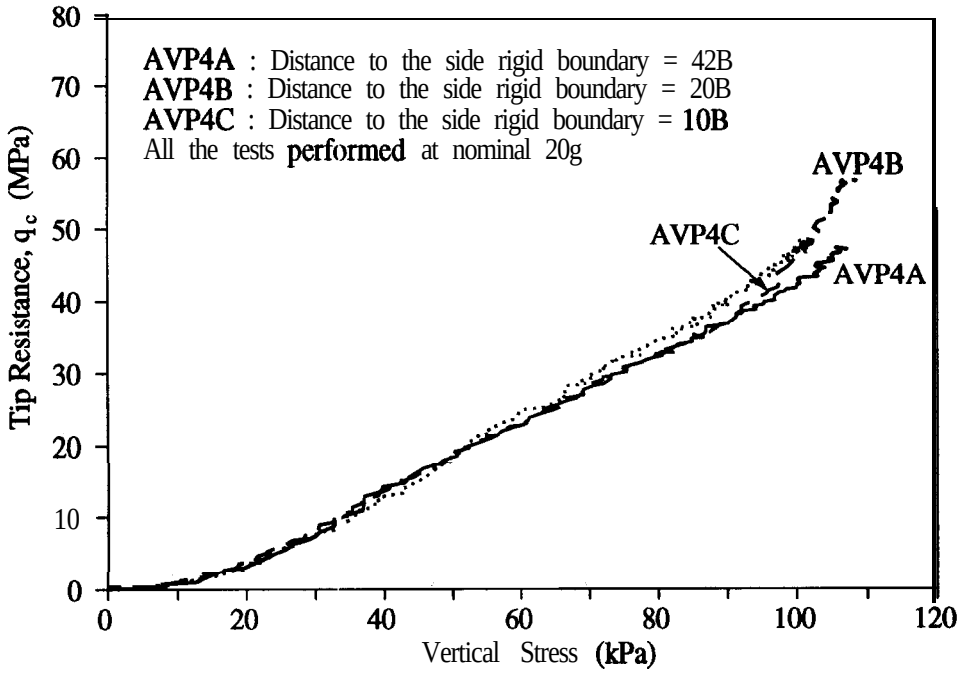

(a) Dense Fontainbleau sand

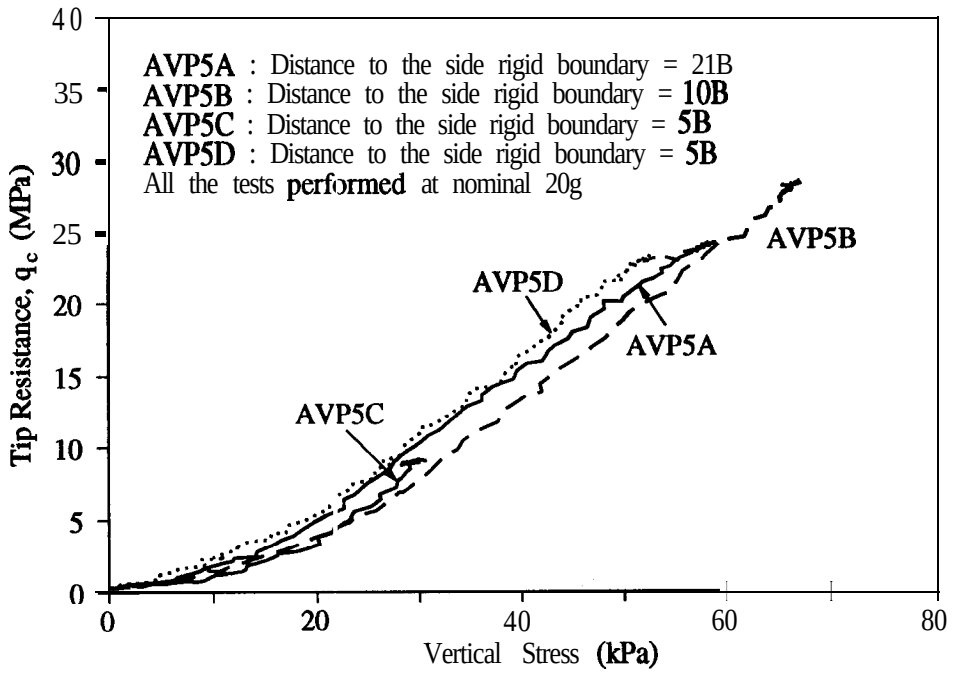

(b) Dense 14/25 Leighton Buzzard sand

Figure 4: Tip resistance profiles (after Phillips and Valsangkar, 1987)

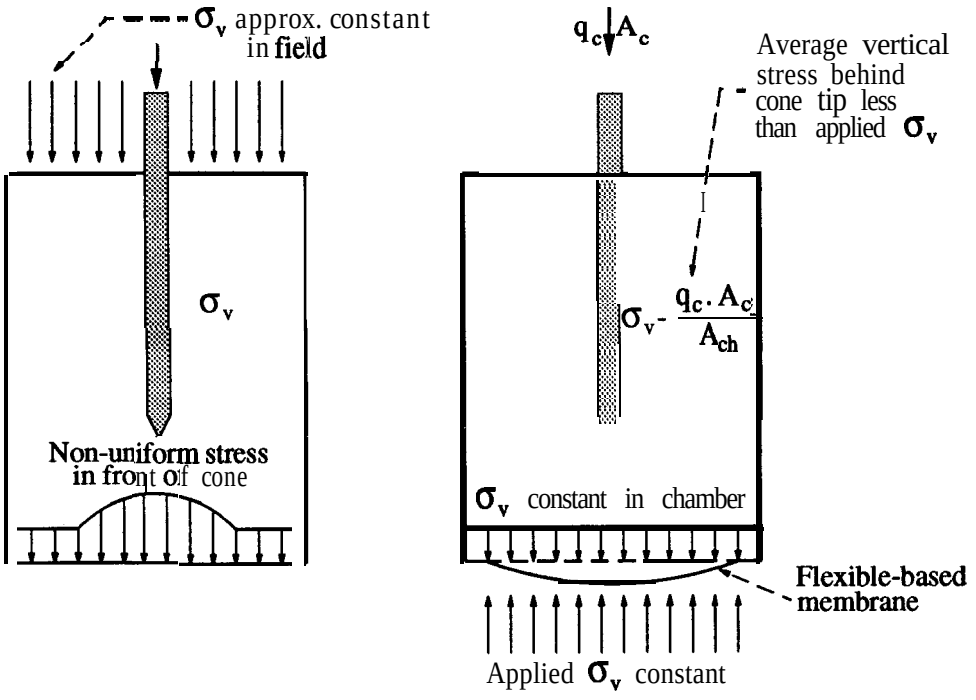

Figure 5: Vertical stress fields around cone in the field and chamber

5. Last (1979) argued that the constant volume boundary condition *B3* does not form a true upper bound of q_c value. The argument was that, the flexible fluid-backed membranes force the boundary to be the principal plane and the mechanism of penetration would be dependent upon the response of the fluid-backed membrane instead of the shear resistance between the sand and the rigid wall. However, Been and Crooks (1988), who interpreted chamber test results in terms of state parameter suggested that this condition will overestimate q_c as compared to field values.

6. Been and Crooks (1988) also concluded that in stress controlled chamber tests, the vertical stresses behind the cone are not constant, but decreases as q_c increases, Fig 5. In the flexible-based chamber tests, the flexibility of the membrane will reduce the stress concentration that can develop in front of the cone. In field or centrifuge tests, the vertical stresses behind the cone are approximately constant and the stress in front of the cone is governed by the soil behaviour.

3 Centrifuge Tests

10 tests were conducted in the centrifuge to study the relative density and boundary effects for CPT. The tests were performed using a cone with diameter B = 10mm and in 3 difference containers with diameter D = 850mm, 420mm and 210mm. The assembled package for centrifuge test and layout of the test location are shown in Fig 6.

3.1 Test programme

The detail and geometry of the tests are tabulated in Table 1.

3.2 Sand properties

Fontainbleau sand, imported from France, was used in the above tests. The particle size distribution has been determined in accordance with BS 1377:1975; clause 2.7.1. The distribution curve is presented in Fig 7.

The measured D_{50} of the Fontainbleau sand is 0.181mm, where D_{50} is the grain diameter at which 50% of the soil weight is finer. D_{60} and D_{10} are 0.191 and 0.113 respectively. Hence, the coefficient of uniformity C_u $(=D_{60}/D_{10})$ of the sand is 1.69. Specific gravity G_s of Fontaibleau sand has also been determined using the method prescribed in BS 1377:1975; clause 2.6.2. The average G_s value is 2.644. These values compared reasonably well to the values obtained by Shi (1988). The sand has a maximum void ratio e_{max} = 0.92 and minimum void ratio e_{min} = 0.55.

3.3 Model preparation

The specimen was prepared by raining the Fontainbleau sand from a single hole hopper into the cylindrical container. The void ratio of the specimen depends on the flow rate and the height of pouring. To achieve a constant void ratio, the height of the hopper and flow rate were maintained constant throughout the preparation of specimen. The top surface of the specimen was then levelled using a suction machine. The repeatability of this technique

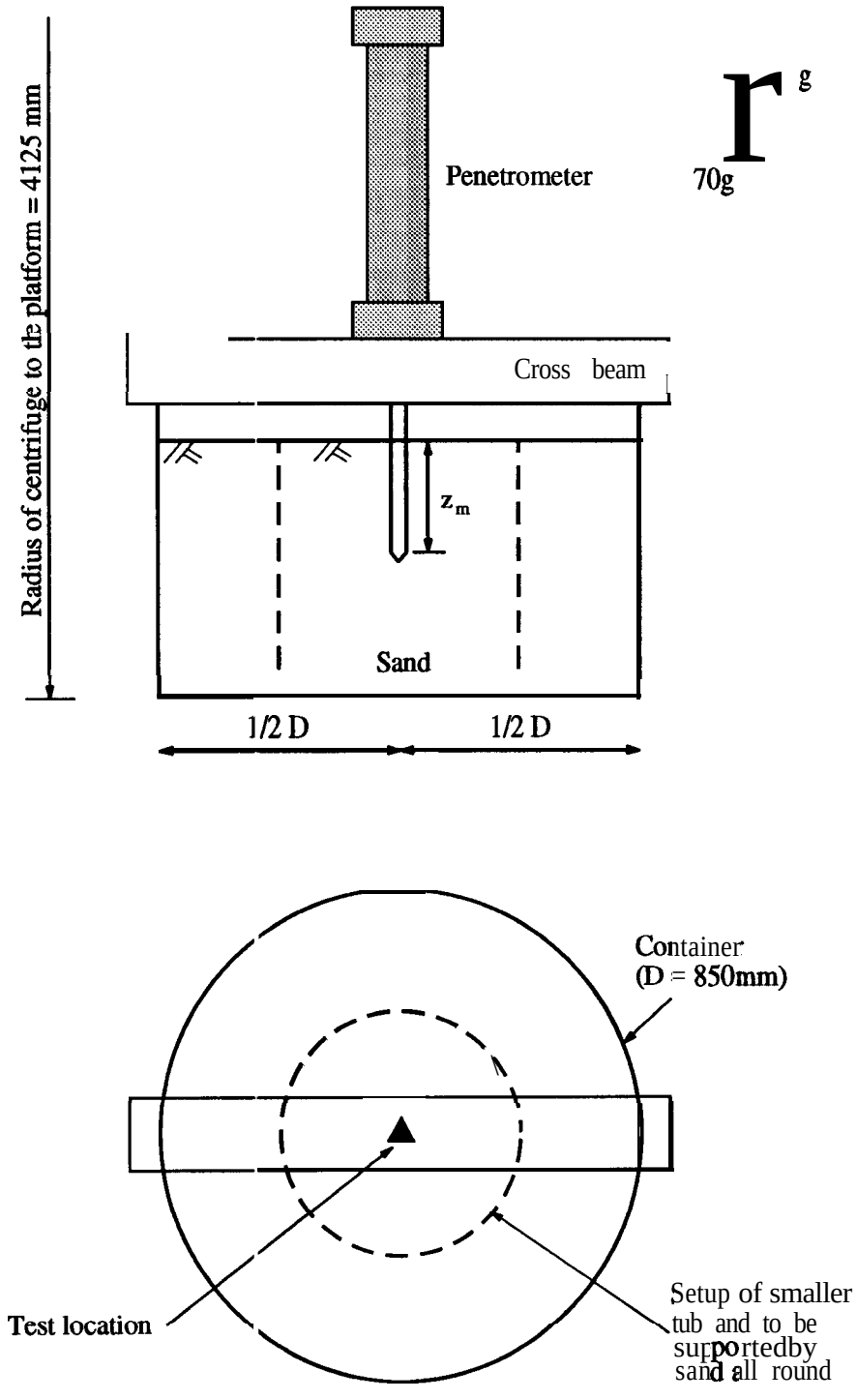

Figure 6: Assembles of centrifuge package

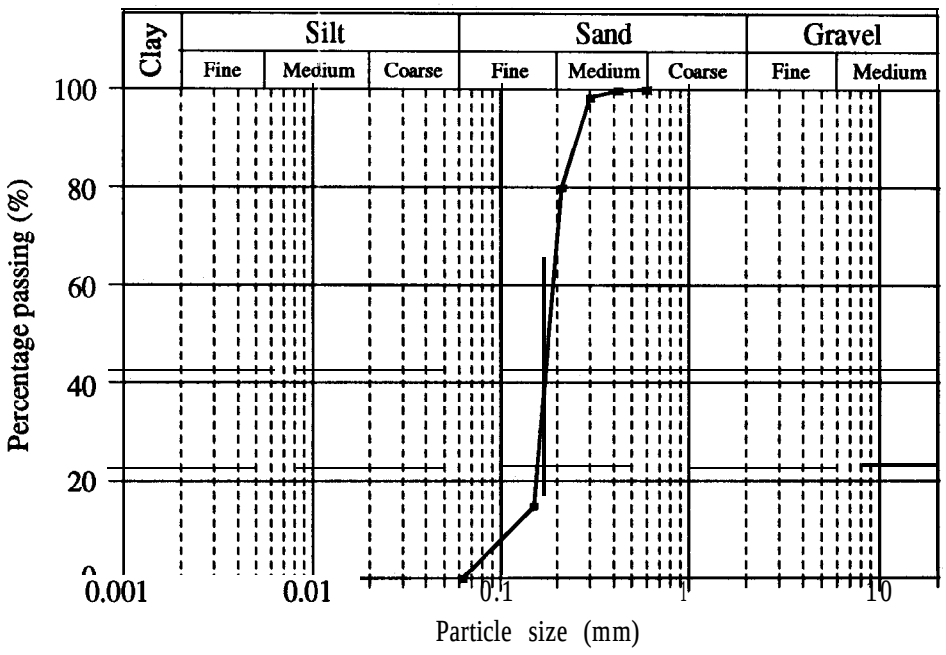

Figure 7: Particle size distribution curve for Fontainbleau sand

is presented in Fig 8. This method of model preparation can also achieve a fairly uniform dense specimen.

To avoid a loose sample densifying when disturbed during handling, the sample was prepared in the centrifuge compound, though shaking as the package goes on the arm is almost bound to cause some densification. Calculation of void ratio is based on the overall weight of the specimen and its volume measured after the package had been mounted on to the centrifuge arm. After each run, the volume of the specimen is measured to ensure that no significant settlement occurred.

3.4 Cone penetration testing

Basically, there are two power systems involved in CPT in the centrifuge.

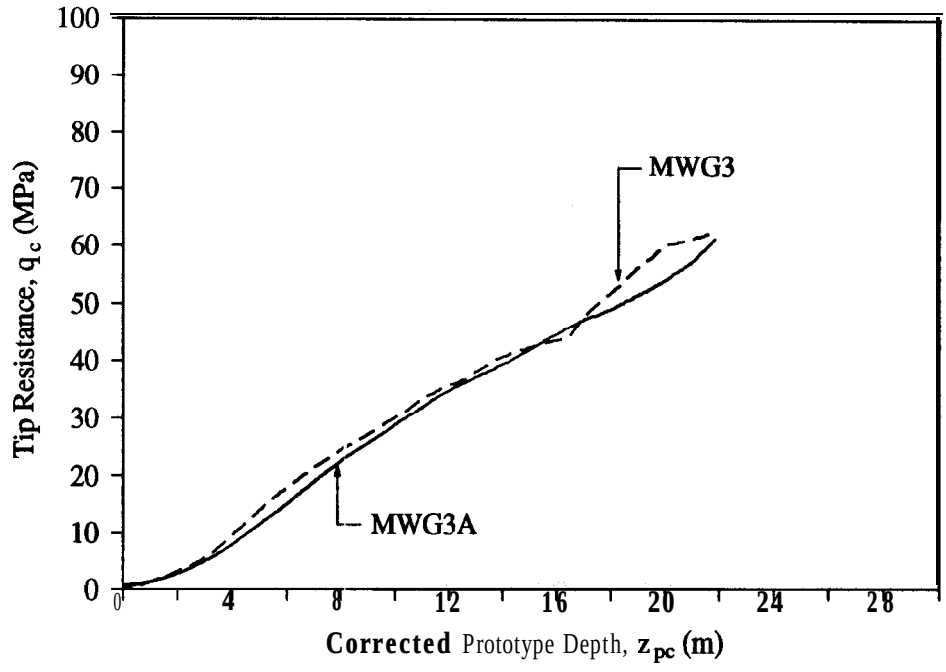

Figure 8: Repeatability of sand pouring technique in Cambridge

3.4.1 Power system - Pneumatic

Before the penetration test, during centrifuge flight, nitrogen pressure acting in the bottom chamber is used to prevent the downward movement of the probe and piston under gravity force, Fig 9. At an acceleration of $70g$, a pressure of about $1200kPa$ is required to counteract the weight of the probe and piston and also the head of water in the external piping. When required, nitrogen can be vented out of the bottom chamber via a pressure relief valve.

3.4.2 Power system - Hydraulic

Fig 10 schematically shows the hydraulic and pressure control systems required during centrifuge operation of the probe. The hydraulic pressure system is depicted in the top left hand corner of Fig **10** . The 9.4 litre accumulator contains 4 litres of pressurised water with additives. By opening the pneumatically actuated 2-way ball valve the pressurised water will be forced into the top chamber of cone penetrometer, pushing the probe into

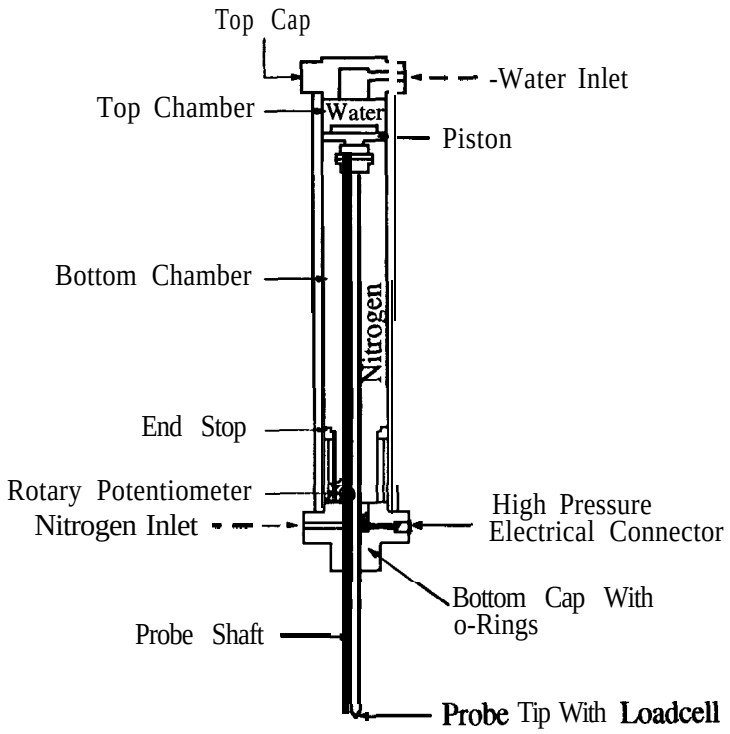

Figure 9: CUED cone penetrometer

the specimen.

When the test was completed and the centrifuge was stopped, the pressure in the accumulator was released. The probe was retracted by increasing the nitrogen pressure into the bottom chamber. The water mixture in the upper chamber is then forced to flow back to the accumulator.

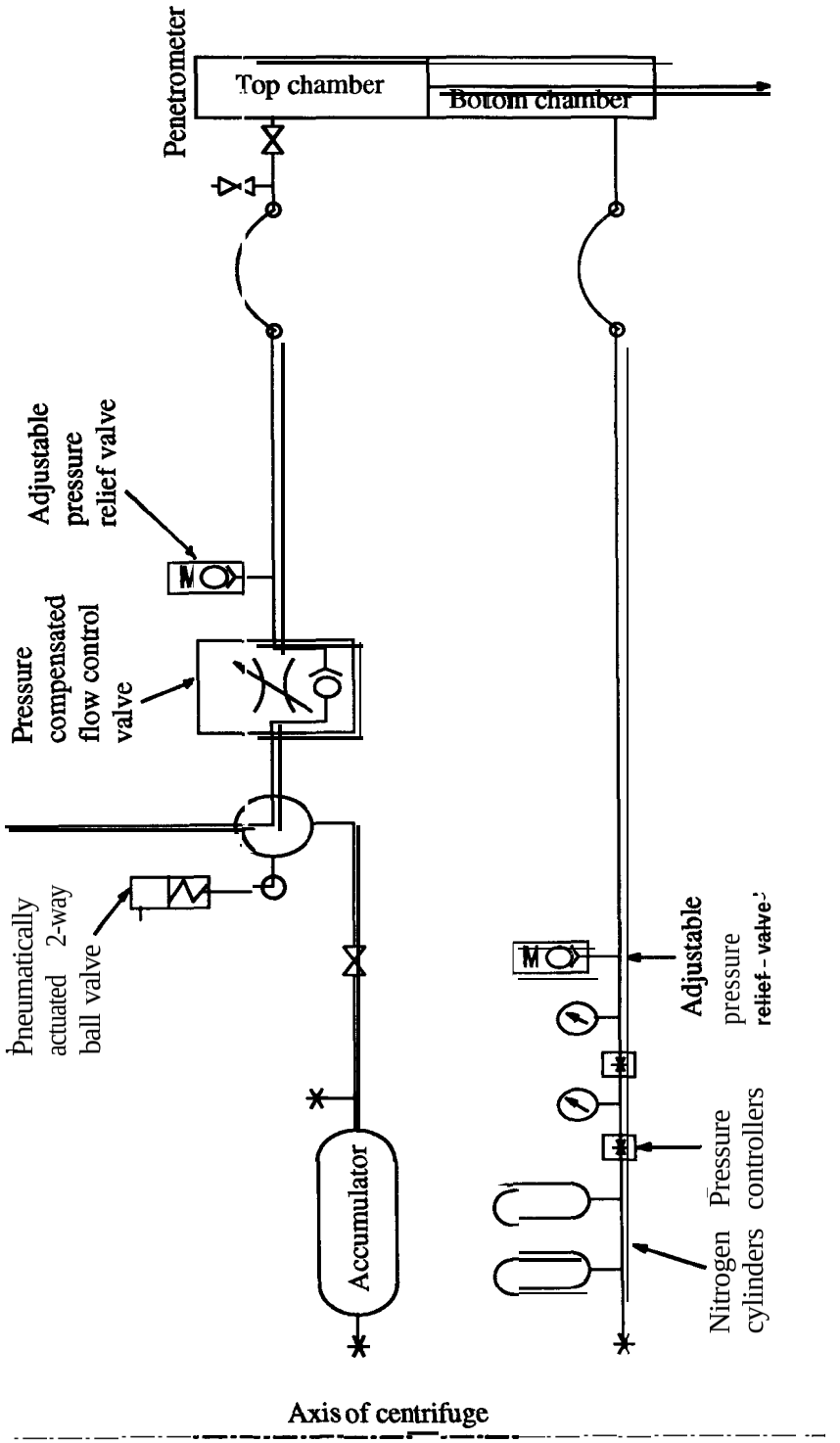

Figure 10: Hydraulic system on centrifuge arm

4 Analysis of Results

Only one CPT was executed for each of the specimen prepared and the location was at the center of the specimen, Fig 6. The results of CPT are then plotted in the following ways :

1. tip resistance q_c versus corrected prototype depth z_{pc}
2. normalized tip resistance Q versus normalized depth of penetration Z

where :

$$z_{pc} = z_p.[1 + (\frac{z_m}{2R_s})]$$
$$Q = \frac{(q_c - \sigma_v)}{\sigma'_v}$$
$$Z = \frac{z_m}{B}$$
$$z_p = n.z_m$$
$$\sigma_v = \gamma.g.z_p.[1 + (\frac{z_m}{2R_s})]$$
$$\sigma'_v = (\gamma - \gamma_w).g.z_p.[1 + (\frac{z_m}{2R_s})]$$

The tip resistance profile for all the tests are plotted in Fig 11 (a) & (b) while the normalised tip resistance profile are plotted in Fig 12 (a) & (b). In all cases, the depth, z_m, is measured from the surface of the test specimens to the shoulder of the cone, Fig 6.

4.1 Penetration mechanisms

From the normalised plot, Fig 12 (a) & (b), itis clear that for a complete penetration, there are two phases of behaviour depending on the depth ratio, $\frac{z_m}{B}$. In the first phase, Q increases with depth in the fashion of shallow foundations until the so-called critical depth (Vesic, 1963), Fig 13. Thereafter, the coefficient seems to hold steady or to fall slightly, which is the characteristic of deep foundations.

The existence of a shallow penetration mechanism requires new correlations in order to analyse the data obtained from centrifuge models. In the calibration chamber tests, this mechanism was omitted since most of the data points were recorded at the mid depth of the sample, well below the critical depth.

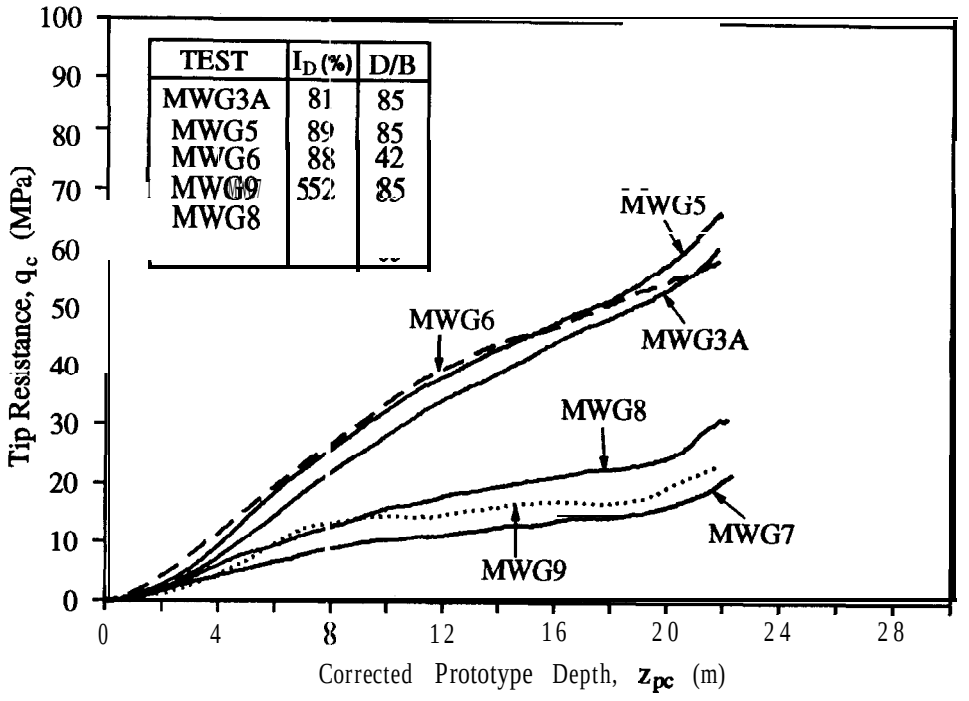

(a)

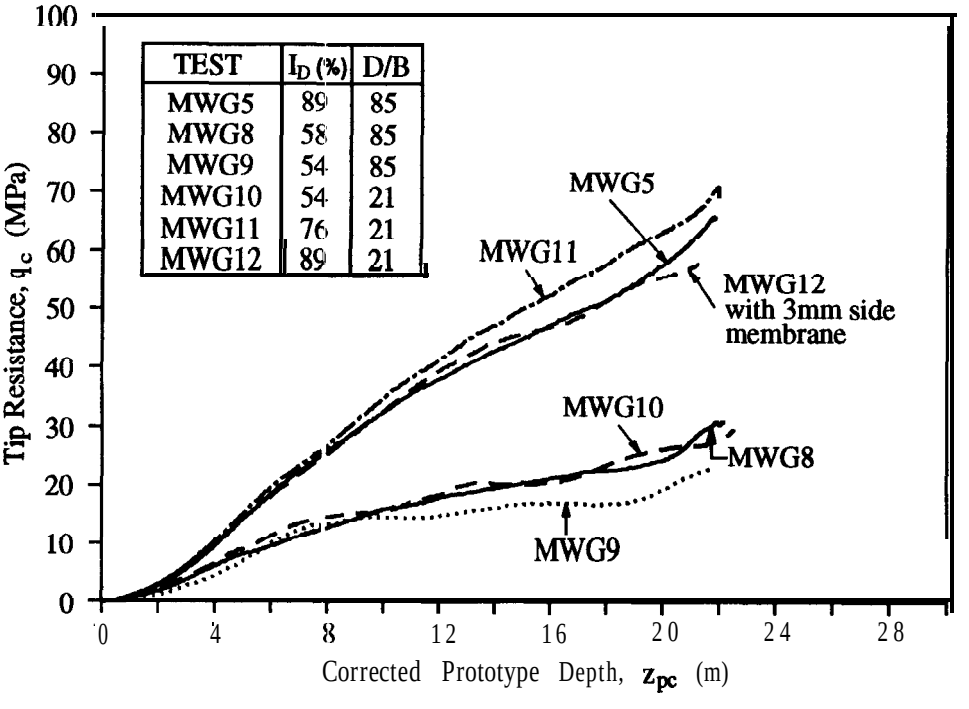

(b)

Figure 11: Tip resistance profiles

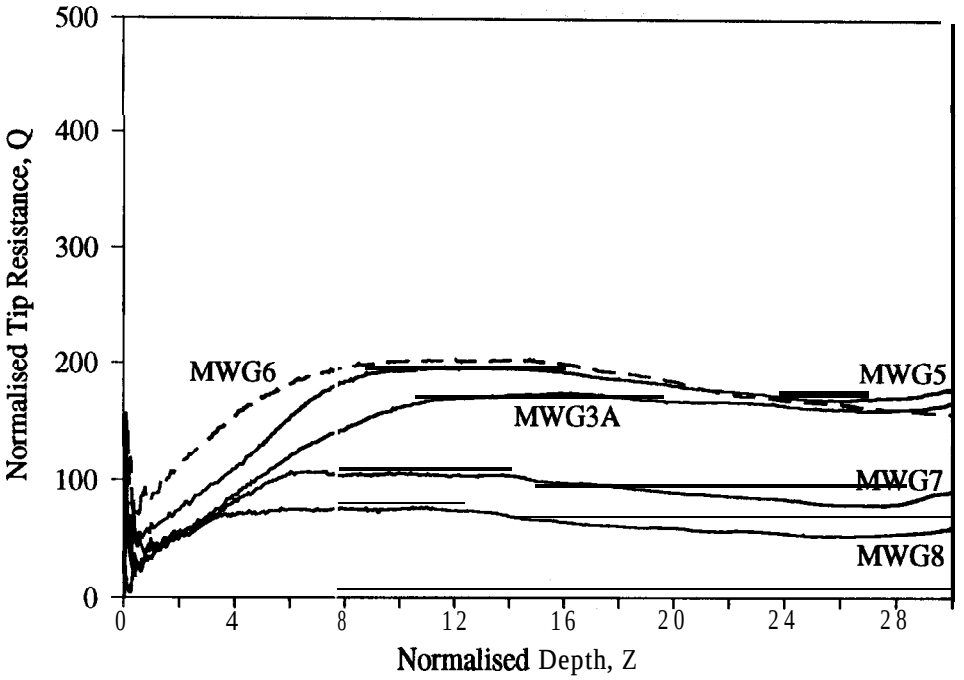

(a)

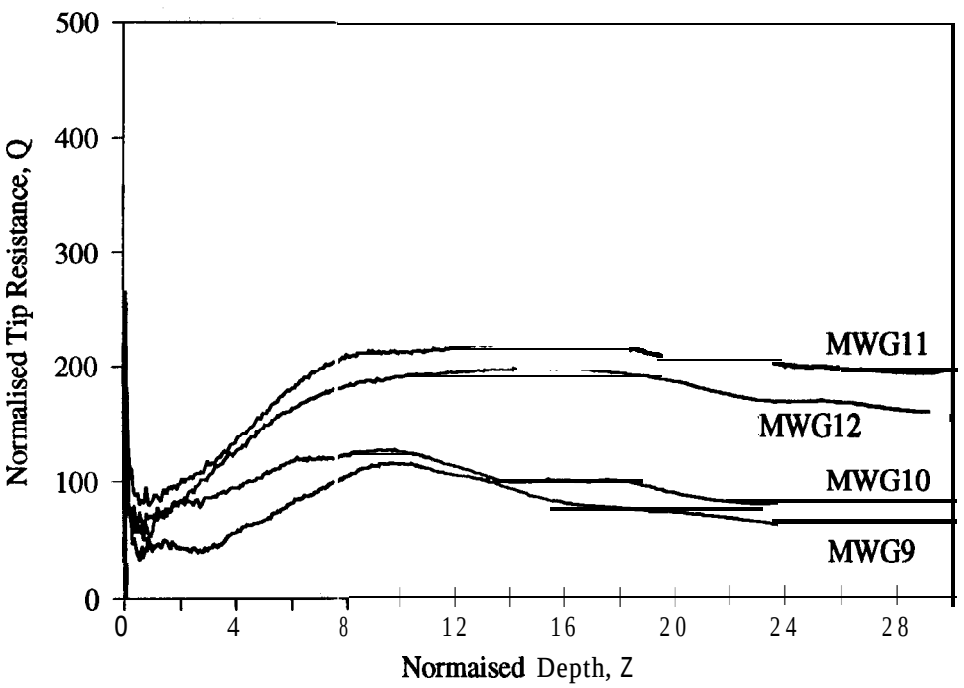

(b)

Figure 12: Normalised tip resistance profiles

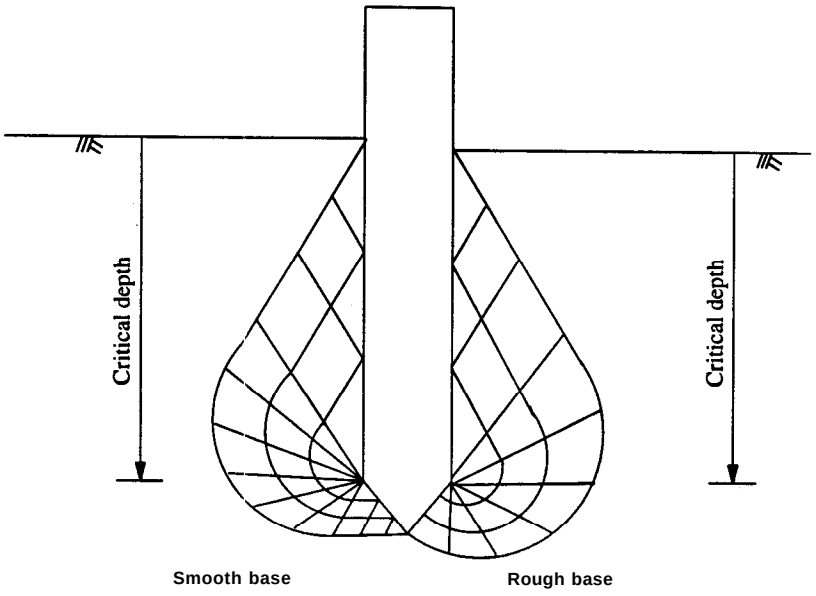

Figure 13: Definition of critical depth

4.2 The effect of relative density, I_D

Fig 11 (a) & (b) show that q_c is significantly affected by I_D. This is because q_c is very much dependent on the mobilised angle of shearing. For a particular stress level, soil with higher density is always associated with higher mobilised angle of shearing. The CPT profile of the specimen reveals it is not easy to achieve a consistent density for a specimen with $I_D < 60\%$.

4.3 The effect of side boundary

In order to study the side boundary effect, q_c is plotted against $\frac{D}{B}$ as in Fig 14 (a) & (b). For very dense Fontainbleau sand specimens, Fig 14(a), there is no apparent increase in q_c for a test done in $\frac{D}{B}$ = 42, as compared to $\frac{D}{B}$ = 85. It should be noted that all the density measurements are accurate to the nearest $\pm 2.0\%$, so we should not be surprised to see that q_c for a nominal density I_D = 88% appears higher than q_c for I_D = 89%. However, Fig 14 (a) shows that q_c rose significantly for a test carried out in container with $\frac{D}{B}$ = 21,

even though I_D = 76%. One may therefore suggest that for dense sand, a minimum $\frac{D}{B} = 40$ is desirable.

Fig 14(b) shows the results obtained from specimens with I_D = 54%. Perhaps, more data are needed in order to study the side boundary effect and also to recommend a minimum diameter ratio. Nevertheless, the extrapolated profile (dotted line) indicates that the increment in q_c is moderate as compared with very dense specimens.

In this case, the failure mechanism was apparently restrainted by the boundary of the smaller container, which resulted in higher q_c. However, the setup of the test by Phillips and Valsangkar (1987) was completely different because the probe was placed at $10B$ (B $= 10mm$) from the side wall of a $850mm$ diameter container. This allowed the failure mechanism to develope freely on the other side of the probe. This Phillips and Valsangkar (1987) mechanism was presumably essentially similar to those generated when the probe was penetrating in the center of a. big tub, except that, it was distorted.

Test MWG12 (I_D = 89%) was conducted in a container with $\frac{D}{B}$ = 21, Fig 11(b) and Fig 14 (a). In order to simulate the infinite body of sand, *a 3mm* thick membrane (E = $2.75N/mm^2$) was placed at the circumference of the container. The q_c profile fell nicely on the profile obtained from test MWG5 (I_D = 89%, $\frac{D}{B}$ = 85), except for the last *3m* of penetration.

Though the boundary was restrained, the volumetric changes due to the insertion of probe will be much higher in this setup than the hard boundary condition since the membrane can be deformed easily. An increment in volumetric change means that the soil is more compressible and it will induce a lower q_c value, Vesic (1972).

4.4 The effect of base boundary

A base boundary effect was detected in most of the tests done in the centrifuge (eg. Phillips and Valsangkar, 1987; Lee, 1990 and Phillips and Gui, 1992). From the above tests, it was found that the base effect is more significant and obvious in dense specimens (I_D > 80%). In order to eliminate the base boundary effect, a *3mm* thick membrane was placed at the base of the test container MWG6 and MWG7.

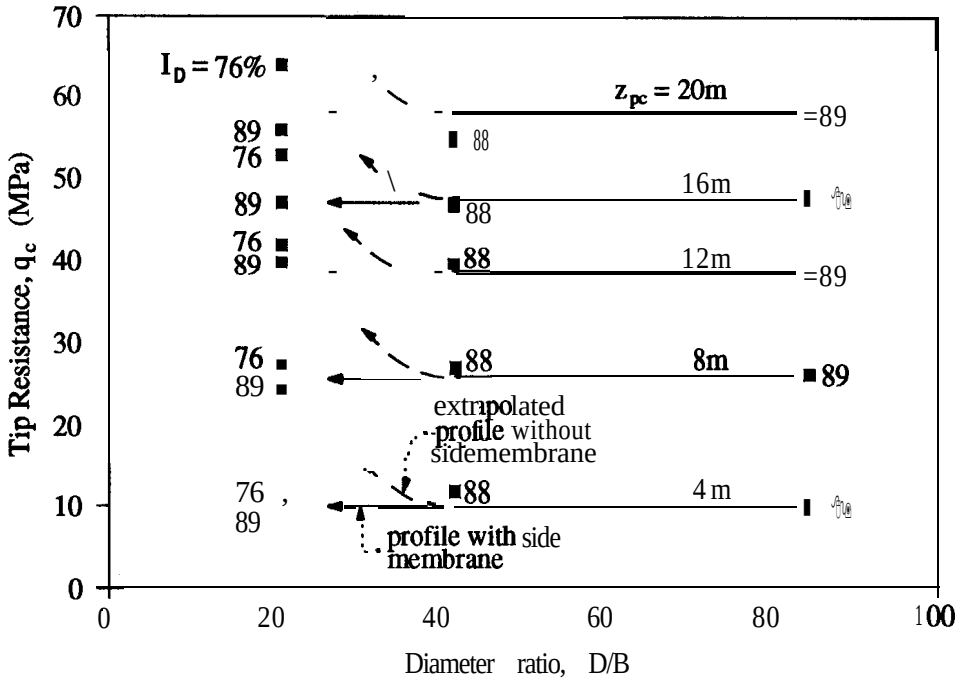

(a)

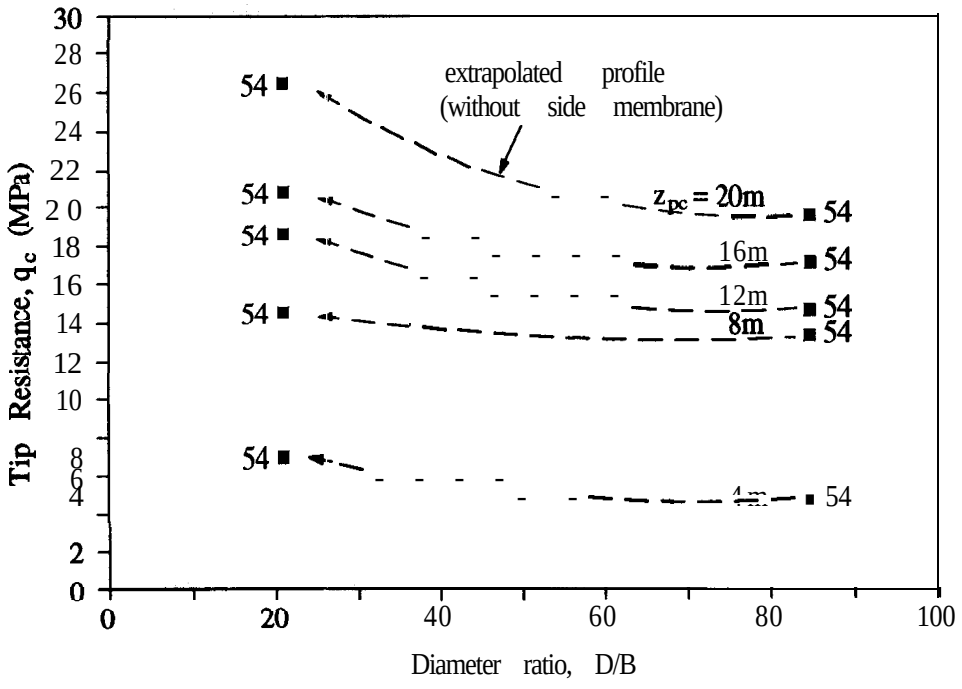

(b)

Figure 14: Relationship between q_c and diameter ratio, $\frac{D}{B}$

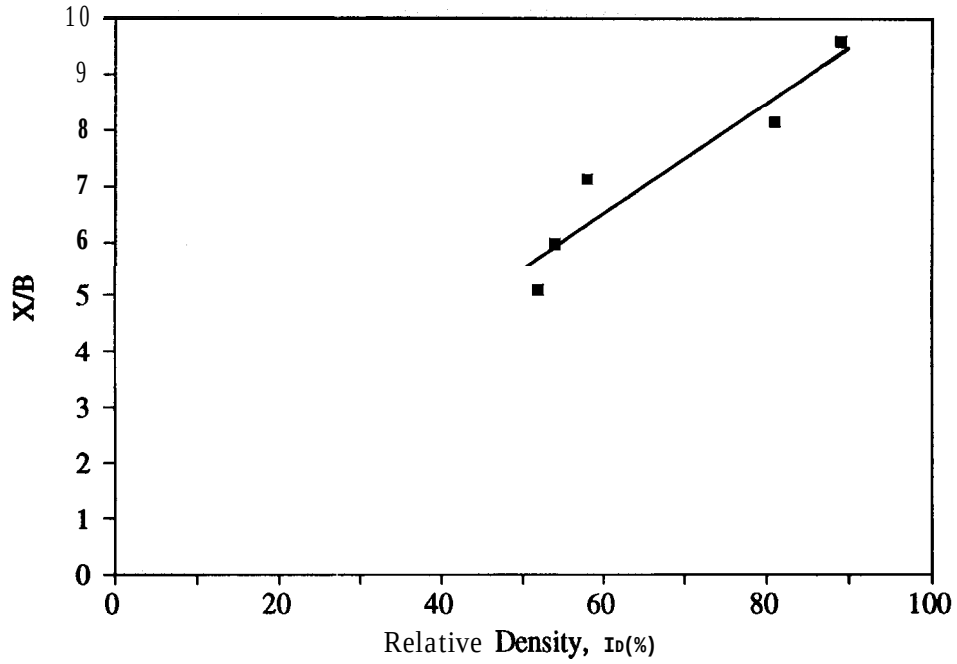

Figure 15: Base boundary effect for Fontainbleau sand @ 70g

From Fig 12(a), it can be observed that the base boundary effect for dense specimen in test MWG6 was not as much as tests MWG3A and MWG5. For loose specimen MWG7 ($I_D < 54\%$), the introduction of a base membrane failed to eliminate the effect. This is because, while the cone is advancing, the loose sand in front of the cone is densifying all the time.

The base boundary effect recorded from the tests was found to be influenced significantly by the relative density of the sand. To find a relationship between these two parameters, $\frac{X}{B}$ is plotted against I_D in Fig 15, where X is the distance from the base of the container to the shoulder of cone.

The best fitted line through these data points suggested that,

$$\frac{X}{B}=0.099(I_D\%) + 0.596 \qquad (1)$$

with the coefficient of correlation, R^2, between the interpolated line and the data points being 0.90.

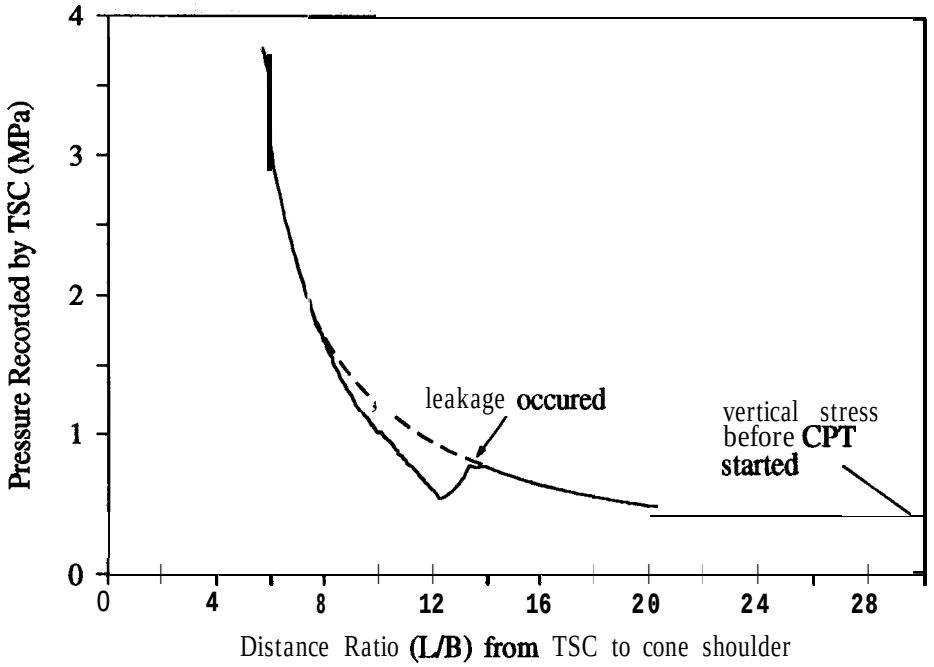

Figure 16: Pressure recorded as the penetrometer advancing

4.5 Base boundary pressure during penetration

Fig 16 shows the pressure recorded while the cone is advancing toward the base of the container. The total stress cell is placed right underneath the cone at the base of the container MWG11 (I_D = 76%). This information is very useful because it shows that the zone of influence of the advancing cone is large. The cell appears to detect the stress induced as soon as the penetration started. This mean that the stress influence bulb induced by the cone can easily reach up to **30B** and this can partly explain why a diameter ratio of **40** is required for the container. It also indicates that there must be very large stress gradient in the sand around the penetrometer since q_c is about $65MPa$ while the recorded pressure at a separation of $6B$ is only about $3MPa$.

It is believed that the sudden dropped in the recorded pressure at about 13B from the base is due to the leakage in the total stress cell. However, the leakage ceased after a while and it continued to register the incremental pressure. The dotted profile in Fig 16 is the assumed profile which is thought to be the correct pressure path.

4.6 Correlation between normalised q_c and I_D

Many researchers (eg. Schmertmann, 1976 and 1978, Jamiolkowski et al. 1985) have proposed empirical correlations between q_c and In. However, all these recommendations were based on the data obtained from calibration chamber tests. The mechanisms of penetration in a calibration chamber and in the centrifuge, as explained earlier, are rather different. Hence, the application of these empirical correlations to centrifuge data has always been unsuccessful. Furthermore, Villet and Mitchell (1981) have demonstrated that there is no single unique relationship that is valid between I_D, q_c and σ'_v, for all sand.

Dimensional analysis proposed by Bolton et al. (1993) reveals that :

$$\frac{q_c - \sigma_v}{\sigma'_v} = N_p\{\phi_{crit}, \frac{\sigma'_v}{p'_c}, OCR, I_D, \frac{z_m}{B}, \frac{B}{d}\} \qquad (2)$$

where ϕ_{crit} and p'_c refer to intrinsic soil properties (angle of shearing resistance at constant volume, and an aggregate crushing parameter, defined by Bolton, 1986); while σ'_v, *OCR* and I_D refer to the current soil state (the initial effective vertical stress, overconsolidation ratio which affects earth pressure coefficient and relative density).

Following the above recommendation, I_D is plotted against normalised tip resistance, $(\frac{q_c - \sigma_v}{\sigma'_v})$, Fig 17. A linear correlation, A, can then be assumed to relate both dimensionless parameters,

$$I_D(\%) = 0.2831(\frac{q_c - \sigma_v}{\sigma'_v}) + 32.964 \qquad (3)$$

but this relation cannot generally be a straight line since some small resistance is always registered even at small relative densities. The grouping of the data does not presently permit a proper evaluation of the true shape of the function (curve B in Fig 17 is not determinable). The linear relationship might, however, estimate I_D of the test specimens for any depth that is greater than the critical depth if I_D lies in the range of 50% to 100%. Stress level effects (Bolton et al. 1993) and the base effect have to be taken into account when applying this equation.

From the calibration chamber tests carried out in uncemented, NC quartz sand, Jami-

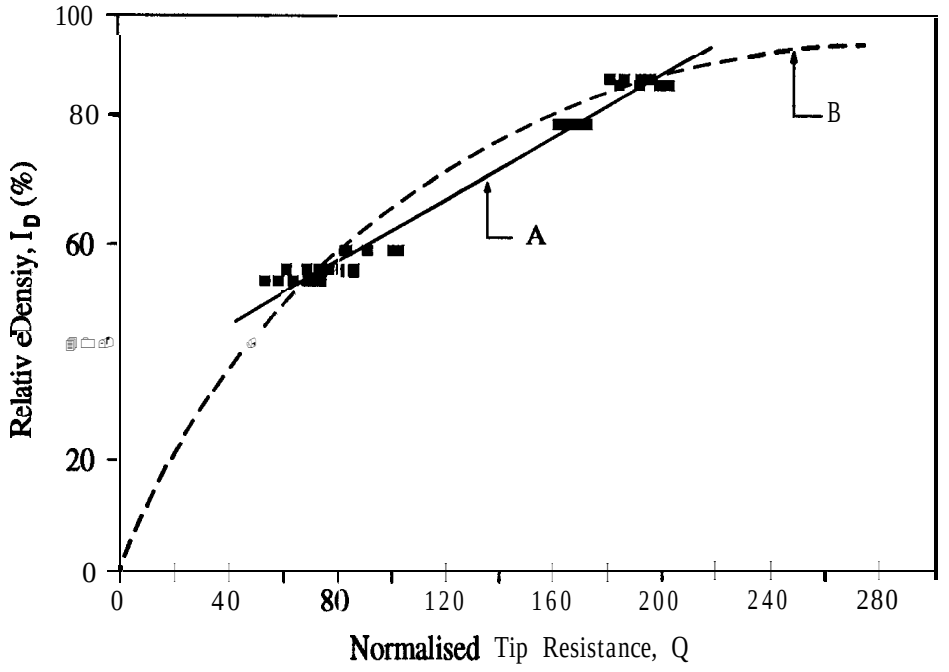

Figure 17: Relationship between I_D and normalised q_c

olkowski et al., (1985) proposed a correlation,

$$ID(\%) = -98 + 66 log \frac{q_c}{[\sigma'_v]^{0.5}} \quad (4)$$

where q_c and σ'_v are expressed in $tonne/m^2$. Fig 18 (a) & (b) show the comparison of the estimated I_D using equation (3) and (4) and centrifuge data. For a particular depth, equation (3) will overestimate and underestimate the I_D by about 6% and 9% respectively, as compared to 10% and 20% if equation (4) was used.

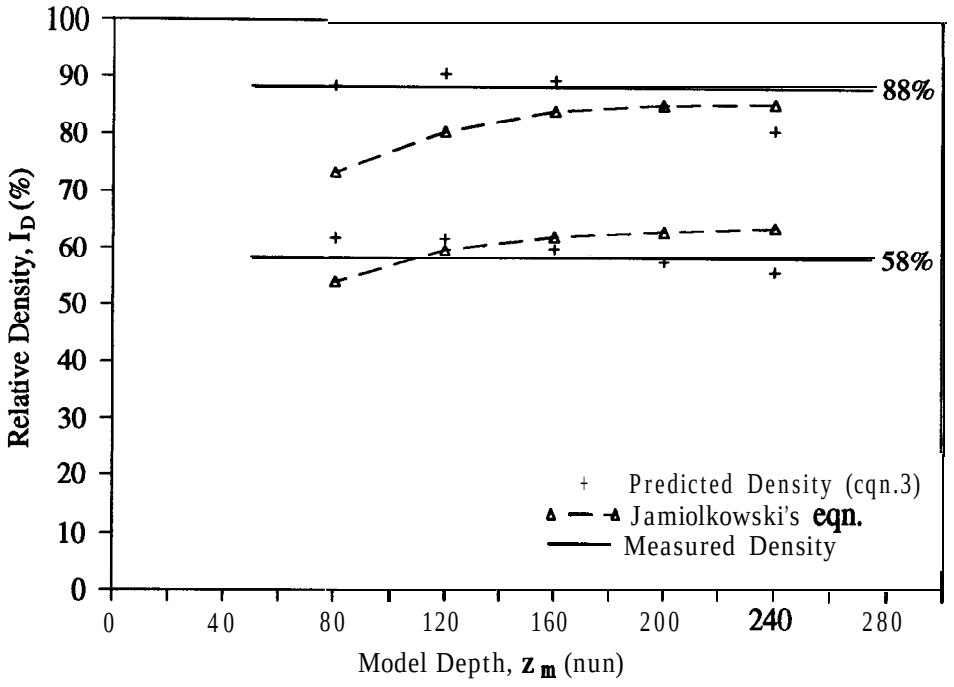

(a)

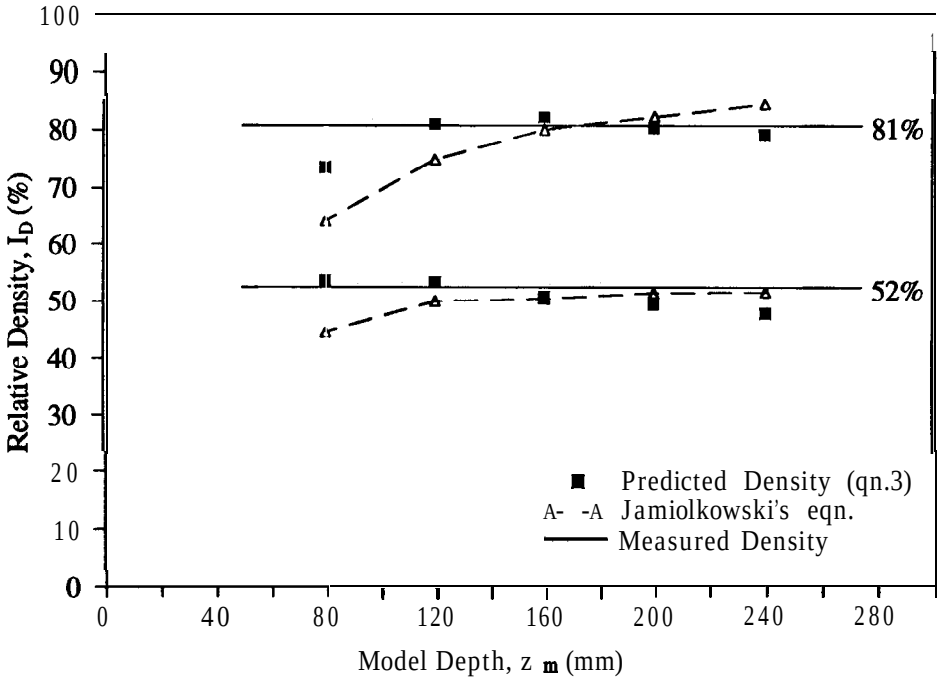

(b)

Figure 18: Comparison of the estimated I_D profiles

5 Conclusion

1. A series of centrifuge tests have been carried out in order to study the influences of diameter ratio and relative density in CPT results. The results observed for side boundary effect confirmed the finding of Last (1979).

2. The measured base boundary pressure during the advancing of the cone indicates the necessity of having a large diameter ratio in order to eliminate the proximity of boundary.

3. Boundary effects depend strongly on the relative density of the soil. In order to prevent the influence of a side boundary in dense samples, a diameter ratio $\frac{D}{B}$ of at least 40 is suggested. However, more tests have to be done in order to find the minimum diameter ratio for loose sample.

4. A rubber membrane of sufficient thickness can be used at the circumference of the smaller container in order to simulate the infinite boundary condition.

5. The base boundary effect also depends on the relative density of the soil and the introduction of base membrane in dense specimen would affect the result obtained particularly when the cone is at $5B$ to $10B$ from the base.

6. Relative density has a significant effect on q_c and can be correlated using equation 3.

7. New correlations are required to analyse the CPT data obtained from the centrifuge, particularly for the shallow penetration mechanism.

Acknowledgement

This study was made possible by the financial support of the European Economic Community - EEC Science Contract SC1-CT91-0626 entitled "Improvement of model testing in the geotechnical field" with Jean-Francois Corté acted as scientific coordinator. The participation of ISMES (Bergamo), RUB (Bochum), DIA (Copenhagen) and LCPC (Nantes) is also acknowledged.

References

1. Been, K. and Crooks, J.H.A (1988). A critical appraisal of CPT calibration chamber tests. Proc. of the Int. Symp. on Penetration Testing 1988, vl, p651-660.

2. Bolton, M.D. (1986). The strength and dilatancy of sands. Geotechnique 36, No 1, p65-78.

3. Bolton, M.D., Gui, M.W. and Phillips, R. (1993). Review of miniature soil probes for model tests. llth.South East Asia Geotech. Conf., Singapore, p85-91.

4. Ferguson, K.A. and Ko, H.Y. (1981). Centrifugal model of the cone penetrometer. Proc. of a Session on Cone Penetration Testing and Experience, ASCE National Convention, St. Louis, Missouri, October, p108-127.

5. Ghionna, V. (1984). Influence of chamber size and boundary conditions on the measured cone resistance. Seminar on CPT in the laboratory, University of Southampton.

6. Jamiolkowski, M. et al. (1985). New developments in field and laboratory testing of soils. Theme Lecture, 11th. Int. Conf. on Soil Mechanics and Foundation Engineering, San Francisco.

7. Last, N. (1979). Cone penetration tests on samples of dry Hokksund sand in a rigid walled chamber. NGI Report No.52108-8.

8. Lee, S.Y. (1990). Centrifuge modelling of cone penetration testing in cohesionless soils. PhD Thesis, Cambridge University, UK.

9. Parkin, A.K. and Lunne, T. (1982). Boundary effects in the laboratory calibration of a cone penetrometer for sand. Proc. of the 2nd. European symp. on Penetration Testing, Amsterdam, v2, p761-767.

10. Phillips, R. and Gui, M.W. (1992). Cone penetrometer testing : Phase I report. In-situ Investigation EEC Contract : SC1-CT91-0676.

11. Phillips, R. and Valsangkar, A.J. (1987). An experimental investigation of factors affecting penetration resistance in granular soils in centrifuge modelling. Technical Report No CUED/D-Soils TR210, Cambridge University, UK.

12. Schmertmann, J.H. (1976). An updated correlation between relative density, D_r and Fugro-type electric cone bearing q_c. Waterways Experiment Station, Vicksburg, Miss. Contract report, DACW 38-76-M 6646. 145p.

13. Schmertmann, J.H. (1978). Guidelines for cone penetration test : performance and design. United State Department of Transportation, Federal Highway Administration Offices of Research and Development, Washington, D.C. Report, TS-78-209. 146p.

14. Shi, Q. (1988). Centrifugal modelling of surface footings subject to combined loading. PhD Thesis, Cambridge University, UK.

15. Vesic, A.S. (1963). Bearing capacity of deep foundations in sand. Highway Research Record No 39, p112-153.

16. Vesic, A.S. (1972). Expansion of cavities in finite soil mass. Jour. of the Soil Mechanics and Foundations Division ASCE, vol 98, No SM3, Proc. paper 8790, p265-290.

17. Villet, W.C.B. and Mitchell, J.K. (1981). Cone resistance, relative density and friction angle. Proc. of a Session on Cone Penetration Testing and Experience, ASCE National Convention, St. Louis, Missouri, October, p178-208.

Table

Test	MWG3	MWG3A	MWG5	MWG6	MWG7
Shape of container[1]	C	C	C	C	C
Size of container (mm)	850	850	850	420	420
Height of spcimen (mm)	350	350	350	350	353
Method of preparation[2]	c	c	c	c	c
Method to estimate dry density [3]	b	b	b	b	b
Estimated dry density (kg/m^3)	1631	1631	1663	1660	1532
Void ratio, e	0.621	0.621	0.590	0.593	0.726
Relative density, I_D(%)	81	81	89	88	52
Level of acceleration at surface	70	70	70	70	70
Radius at the surface of the sand (mm)	3763	3763	3755	3752	3749
Diameter of cone (mm)	10	10	10	10	10
Distance from the wall (cone diameter)	42.5	42.5	42.5	21	21
Rate of penetration (mm/s)	4.1	3.8	3.6	3.3	3.3

Test	MWG8	MWG9	MWG10	MWG11	MWG12
Shape of container[1]	C	C	C	C	C
Size of container (mm)	850	850	210	210	210
Height of spcimen (mm)	351	348	358	351	342
Method of preparation[2]	c	c	c	c	c
Method to estimate dry density [3]	b	b	b	b	b
Estimated dry density (kg/m^3)	1552	1538	1538	1613	1662
Void ratio, e	0.704	0.719	0.719	0.639	0.590
Relative density, I_D(%)	58	54	54	76	89
Level of acceleration at surface	70	70	70	70	70
Radius at the surface of the sand (mm)	3751	3757	3747	3754	3763
Diameter of cone (mm)	10	10	10	10	10
Distance from the wall (cone diameter)	42.5	42.5	10.5	10.5	10.5
Rate of penetration (mm/s)	3.5	3.5	3.7	3.7	3.7

Table 1

where,

1. R : Rectangular; C : Cylindrical

2. a : travelling pluviation in air;
   b : rotating pluviation in air;
   c : pluviation in air from a single hole hopper

3. a : local measurements by calibrated boxes placed at the bottom;
   b : measurement of the total mass

Note that membranes were used in the following test :

1. A 3 mm thick rubber (E = 2.75 N/mm^2) was introduced at the base of the container in test MWG6 and MWG7.

2. A 3 mm thick side membrane was introduced in test MWG12.